

JOURNAL OF THE AMERICAN CHEMICAL SOCIETY

Trifluoroethanol Drives Platelet Factor 4 Subunit Association Rate toward the Smoluchowski–Stokes–Einstein Dynamic Diffusion Limit

Sharon Barker and Kevin H. Mayo*

Contribution from the Structural Biology Group, Jefferson Cancer Institute, Blumerle Life Sciences Building, Room 815, Thomas Jefferson University, 1020 Locust Street, Philadelphia, Pennsylvania 19107. Received May 16, 1991

Abstract: Under certain solution conditions, platelet factor 4 (PF4) monomers (7800 Da), dimers, and tetramers exist in solution in slow exchange on the ^1H NMR (500 MHz) time scale (Mayo, K. H.; Chen, M. J. *Biochemistry* **1989**, *28*, 9469). In the presence of increasingly low concentrations of trifluoroethanol (less than 1–5%), the normally observed slow monomer–dimer–tetramer exchange is driven into an intermediate and then fast chemical exchange regime. This indicates that PF4 subunit exchange rates are dramatically increased to in excess of 1000 s^{-1} . While other chemical agents are known to dissociate aggregate states, trifluoroethanol is unusual in that it enhances protein molecular association rates. In the slow and slow–intermediate exchange regimes, association/dissociation kinetic parameters have been derived from exchange-induced line width increases. In the absence of trifluoroethanol, the PF4 monomer association jump rate is 18 s^{-1} ($1.6 \times 10^5\text{ M}^{-1}\text{ s}^{-1}$), which is about 3–4 orders of magnitude below the traditionally derived Smoluchowski–Stokes–Einstein theoretical rate of diffusional encounter. When PF4 subunit exchange is brought into the NMR fast exchange regime, i.e., 1000 s^{-1} and above, trifluoroethanol effectively has driven PF4 subunit association toward this theoretical dynamic diffusion limit.

Introduction

Human platelet factor 4 (PF4), a secretory peptide from α -storage granules, contains 70 amino acid residues^{1–4} of which only three are aromatic, i.e., His 23, His 35, and Tyr 60. PF4 monomers are known to associate in a tetrameric structure at low concentration ($50\text{ }\mu\text{g/mL}$) under physiological conditions^{5,6} and in a distribution of monomer–dimer–tetramer states at higher concentration (mg/mL) under which conditions monomer–dimer–tetramer (M–D–T) equilibria (slow exchange regime on the ^1H NMR time scale) have been investigated by ^1H NMR spectroscopy.⁷ Chen and Mayo⁸ also showed that kinetic exchange parameters for PF4 association/dissociation can be derived from analysis of resonance exchange broadening and saturation transfer–NMR experiments. PF4 subunit association/dissociation exchange jump rates are in the 3–40- s^{-1} range with corresponding rate constants for monomer–monomer and dimer–dimer association of 1.6×10^5 and $0.9 \times 10^5\text{ M}^{-1}\text{ s}^{-1}$, respectively.

Due to a simple downfield aromatic resonance region, reasonably resolved Y60 3,5 proton resonances in monomer, dimer, and tetramer states, and equilibrium exchange fluxes falling into the appropriate NMR time window for slow–intermediate exchange, PF4 is exceptional as an ideal model system for studying solution effects on steady-state kinetics of protein interactions. In many biological processes, the initial reaction step is a diffu-

(1) Deuel, T. F.; Kein, P. S.; Farmer, M.; Heinrichson, R. L. *Proc. Natl. Acad. Sci. U.S.A.* **1977**, *74*, 2256–2258.

(2) Deuel, T. F.; Senior, R. M.; Chuang, D.; Griffin, G. L.; Heinrichson, R. L. *Proc. Natl. Acad. Sci. U.S.A.* **1981**, *78*, 4584–4587.

(3) Hermodson, M.; Schmer, G.; Kurachi, K. *J. Biol. Chem.* **1977**, *252*, 6276–6279.

(4) Walz, D. A.; Wu, V. Y.; de Lamo, R.; Dene, H.; McCoy, L. E. *Thromb. Res.* **1977**, *11*, 893–898.

(5) Barber, A. J.; Kaser-Glanzmann, R.; Jakabova, M.; Luscher, E. F. *Biochim. Biophys. Acta* **1972**, *286*, 312–329.

(6) Moore, S.; Pepper, D. S.; Cash, J. D. *Biochim. Biophys. Acta* **1975**, *37*, 379–384.

(7) Mayo, K. H.; Chen, M. J. *Biochemistry* **1989**, *28*, 9469–9478.

(8) Chen, M. J.; Mayo, K. H. *Biochemistry* **1991**, *30*, 6402–6411.

* To whom correspondence should be addressed.

sional encounter of one protein molecule with another. Often, this rate of diffusion is discussed within the context of the Smoluchowski theory⁹ wherein reaction partners are assumed to be spherical with uniform, instantaneously reactive surfaces.¹⁰ For a protein molecule the size of monomer platelet factor 4 (PF4), i.e., 7800 Da, the hard-sphere (Stokes-Einstein) Smoluchowski theory yields a bimolecular rate constant, k , of about 10^8 – 10^9 M⁻¹ s⁻¹. Most protein-protein bimolecular rate constants are 3–4 orders of magnitude below this value, and PF4 monomer-monomer association is no exception with an association rate constant⁸ of 1.6×10^5 M⁻¹ s⁻¹. This paper gives a unique example of the effect of an organic solvent, trifluoroethanol (TFE), on protein subunit exchange kinetics. TFE has the effect of driving PF4 association dynamics toward the Smoluchowski-Stokes-Einstein diffusion limit.

Methods and Materials

Isolation of PF4. Outdated human platelets were obtained from the Red Cross and centrifuged at 1000g for 1 h to obtain platelet-poor plasma. This preparation was applied to a heparin-agarose (Sigma) column (bed volume 50 mL); the column was washed with 0.2, 0.5, 1, and 1.5 M NaCl. The fraction eluting at 1.5 M NaCl, which yielded most of the PF4,¹¹ was then desalted by dialysis (0.2% trifluoroacetic acid). The resulting solution was concentrated by lyophilization. From about 50 units of outdated platelets, 15 mg of PF4 generally result.

Protein Concentration. Protein concentration was determined by the method of Lowry et al.,¹² and results were calculated from a standard dilution curve of human serum albumin. An alternative method used to determine PF4 concentration was that of Waddell.¹³

Nuclear Magnetic Resonance (NMR) Spectroscopy. Samples for ¹H NMR measurements had been lyophilized and redissolved in ²H₂O immediately before the experiment. The final protein concentration ranged from 1 to 4 mg/mL as indicated in the text. The p²H was adjusted by adding microliter increments of NaO²H or ²HCl to a 0.6-mL sample. All measurements were done at the p²H value indicated in the text read directly from the pH meter and not adjusted for isotope effects.

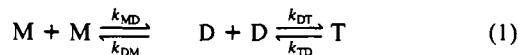
¹H NMR spectra were recorded in the Fourier mode on a General Electric GN-omega-500 NMR spectrometer (500 MHz for protons). The solvent deuterium signal was used as a field-frequency lock. All chemical shifts are quoted in parts per million (ppm) downfield from sodium 4,4-dimethyl-4-silapentanesulfonate (DSS).

Gaussian/Lorentzian Line-Shape Analysis. Resonance area integrals were derived by Gaussian/Lorentzian line fitting of NMR spectra. These procedures were done on a Sun Sparc workstation with standard Gaussian/Lorentzian functions. A part of the NMR spectrum containing the frequency region of interest was transferred to the workstation. Initially, chemical shifts and line widths were taken for the monomer resonance acquired at low PF4 concentration and low pH where greater than 90% monomer state exists;⁷ for the tetramer resonance, a higher protein concentration was used where the tetramer state predominates.⁷ Initial resonance heights were estimated from the position of monomer, dimer, and tetramer resonances, which were generally distinguishable. A base line was established by comparing fits with the noise level where no resonances were found on both sides of the aromatic resonance region. Base lines were generally flat. Derived areas from these fits varied from sample to sample by no more than about 10%.

Half-height line widths, $\Delta\nu_{1/2}$, were estimated from Gaussian/Lorentzian lines fitted to M-, D-, and T-Y60 (3,5) ring proton resonances described above. In cases where resonances did not overlap appreciably, half-height line widths were estimated directly from NMR resonances on the GN-omega-500 spectrometer display.

Results

Platelet factor 4 subunit association/dissociation equilibria can be depicted as shown in eq 1 and as discussed by Mayo and Chen⁷ and Chen and Mayo,⁸ where M, D, and T stand for monomer, dimer, and tetramer, respectively. Steady-state exchange rate



dimer, and tetramer, respectively. Steady-state exchange rate

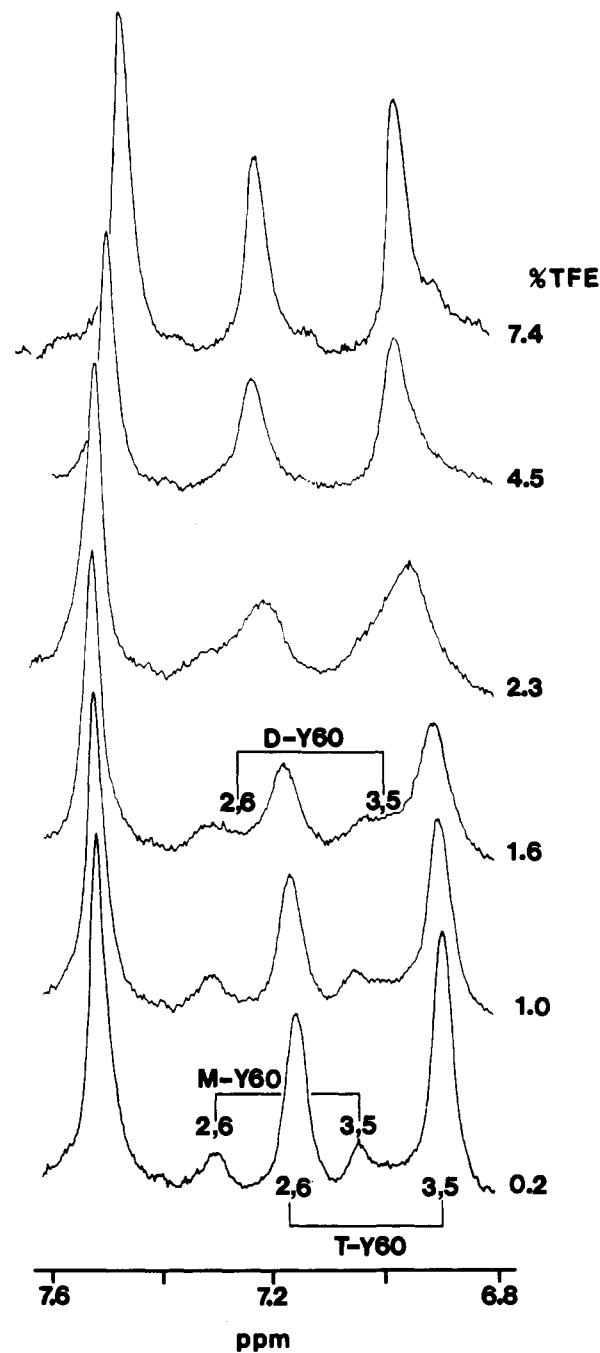


Figure 1. PF4 proton NMR spectra as a function of TFE concentration. 500-MHz proton NMR spectra of human PF4 are shown as a function of percent (v/v) trifluoroethanol as indicated at the right of each spectrum. Lyophilized PF4 sample was dissolved in ²H₂O at pH 3.2, 313 K, containing 6 mg/mL PF4. The only salt added came from the minimal amount of NaO²H and ²HCl necessary to adjust the solution pH; this NaCl concentration was about 10 μ M. No additional buffer or salt was added to these solutions. The resonance label prefixes M, D, and T stand for monomer, dimer, and tetramer, respectively, according to Mayo and Chen.⁷

constants or "jump rates" (inverse lifetime of M, D, or T state) are indicated by k with subscripts for the exchange direction, e.g., MD for monomer to dimer. It has been shown by Mayo and Chen⁷ that, under certain solution conditions, populations of PF4 monomers, dimers, and tetramers exist in slow exchange on an NMR time scale. Moreover, resonances for Y60, H23, and H35 have been identified and assigned to specific M, D, and T aggregate states.⁷

Figure 1 (bottom) shows Y60 2,6 and 3,5 ring proton resonances predominantly from monomer and tetramer states. Conditions were chosen so as to attenuate dimer resonance populations that

(9) von Smoluchowski, M. *Z. Phys. Chem. (Leipzig)* **1917**, *92*, 129–168.

(10) Cantor, C. R.; Schimmel, P. R. *Biophysical Chemistry, Part III*; Freeman: San Francisco, 1980.

(11) Rucinski, B. S.; Niewiarowski, S.; James, P.; Walz, D. A.; Budzynski, A. *Z. Blood* **1979**, *53*, 47–62.

(12) Lowry, O. H.; Rosbough, N. J.; Fan, A. L.; Randall, R. J. *J. Biol. Chem.* **1951**, *193*, 265–270.

(13) Waddell, W. J. *J. Lab. Clin. Med.* **1956**, *48*, 311–314.

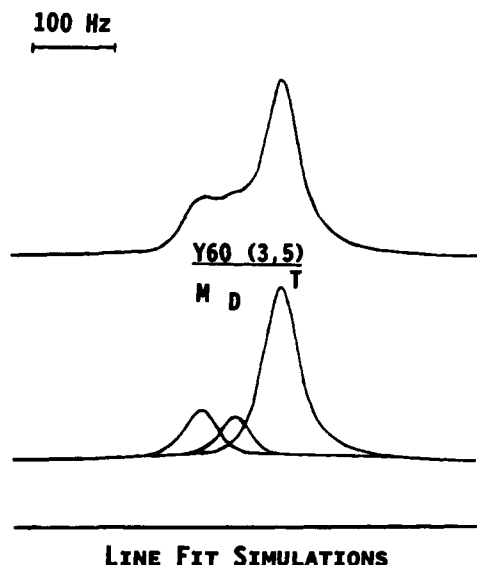


Figure 2. Line fit simulation. For the spectrum shown in Figure 1 at 1.6% TFE, line fit simulations for Y60 3,5 monomer-dimer-tetramer resonances using three Lorentzians are shown at the bottom of the figure. The sum of all Lorentzians is shown at the top of the figure.

would normally appear between monomer and tetramer resonances.⁷ In this way, attention can be focused on the monomer-monomer association and tetramer dissociation processes. Steady-state M- and T-PF₄ populations were derived from Gaussian/Lorentzian fitting of relatively well-resolved M- and T-Y60 2,6 and 3,5 ring proton resonances labeled in Figure 1. Half-height resonance line widths were also estimated from these fits.

The case of slow PF₄ subunit exchange shown at the bottom of Figure 1 is modified by addition of TFE even at concentrations below 1% (v/v). This is evidenced by chemical shift changes and increased exchange line broadening for both monomer and tetramer resonances. In fact, by 3% TFE, monomer and tetramer resonances have coalesced into one highly broadened resonance (intermediate exchange), followed by resonance narrowing as the TFE concentration is further increased (fast exchange limit). In chemical exchange terms, the effect of TFE is to drive PF₄ subunit exchange rates into the fast exchange regime, i.e., on the order of 1000 s⁻¹. Implicit in this qualitative observation is the fact that monomer-monomer association rates are drastically increased. At 7.4% TFE, two minor resonances upfield of Y60, 2,6 and 3,5 resonances become apparent. 2D NMR COSY spectra (data not shown) indicate that these minor resonances are spin coupled and are probably due to a new Y60 state in PF₄, which is induced by higher TFE concentrations. Although its chemical shift is between those of the previously identified dimer and tetramer states,⁷ it is unclear at present to what this state is due. Since at low TFE concentrations this state is not observable, nor is it apparently shifted upfield from the main Y60 resonance during the titration, we shall assume that it is the product of higher TFE concentrations and not consider it further in this paper.

Interestingly, a significant dimer population can be observed by 1.6% TFE. This is made more apparent in the line fit simulation shown in Figure 2. The bottom trace shows three Lorentzians used to fit the monomer-dimer-tetramer Y60 3,5 resonances, while the top trace gives their sum, which can be compared to the spectral trace in Figure 1. The increase in dimer population indicates not only that PF₄ subunit exchange rates are affected by the addition of TFE but that aggregate equilibrium constants, i.e., the ratio of association and dissociation rate constants, are also affected. Steady-state populations in the slow-to-intermediate exchange regime are shifted in favor of monomer and dimer states at the expense of the tetramer state. The actual tetramer resonance area decrease that is observable in the slow to slow-intermediate exchange regime is 10–20%. In the intermediate to fast exchange regimes, direct information on aggregate

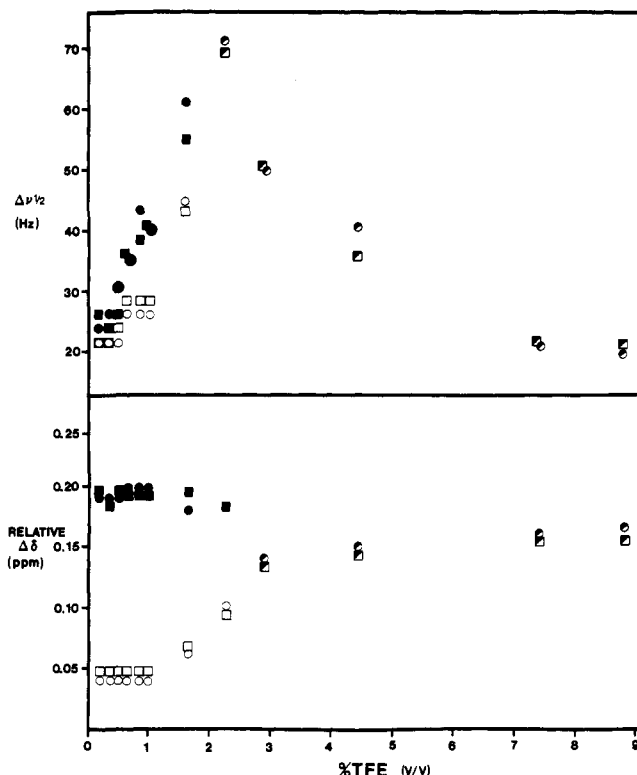


Figure 3. Chemical shift and line width versus TFE concentration. The relative chemical shift change, $\Delta\delta$, and line width half-heights, $\Delta\nu_{1/2}$, of monomer and tetramer Y60 2,6 and 3,5 ring proton resonances is plotted versus the percent (v/v) trifluoroethanol added to the protein solution. Line width half-heights were estimated from actual NMR spectra or from line-shape analyses as described in Methods and Materials. Open symbols refer to the tetramer state, while blackened symbols refer to the monomer state. Squares and circles stand for Y60, 2,6 and 3,5 ring proton resonances, respectively. In cases where monomer and tetramer state resonances overlapped, half-filled symbols are used. For relative chemical shift changes, $\Delta\delta$, a larger number indicates a more downfield chemically shifted resonance.

gate-state populations is lost, but on the basis of continued downfield shifting, i.e., toward the monomer state chemical shift of the fast-exchanging M-D-T Y60 resonances (Figure 3), it appears that this trend continues.

Figure 3 plots monomer and tetramer Y60 2,6 and 3,5 ring proton resonance chemical shift (relative shift differences) and half-height line width changes as a function of percent TFE (v/v) added. It can be noticed that line width and chemical shift changes correlate. An apparent transition point in the titration occurs at about 2% (or 0.2 M) TFE. Monomer Y60 resonances are upfield chemically shifted, while tetramer Y60 resonances are downfield chemically shifted. In cases of nearly equal exchanging populations, this observation is to be expected on going from slow to fast exchange.¹⁴ Remember that, in terms of the tetramer state, Y60 resonance areas must be divided by 4 (subunits) in order to compare equilibrium concentrations in each state.

In cases of moderately slow exchange, resonance lines are broadened by an amount proportional to the steady-state flux rate out of the state observed, i.e., inverse of the lifetime of that state.¹⁴ Since monomer and tetramer Y60 3,5 resonances can be observed in the absence (greater than 90–95%) of other aggregate species by varying PF₄ concentration,^{7,8} it is comparatively evident that considerable resonance broadening occurs in both monomer and tetramer resonances shown in Figure 1. A mathematical expression relating increased resonance broadening and exchange jump rates is shown, for example, in eq 2 where $\Delta\nu_{1/2}^M$ is the

$$\pi(\Delta\nu_{1/2}^M - \Delta\nu_{1/2}^T) = k_{MD} \quad (2)$$

(14) Jardetzky, O.; Roberts, G. C. K. *NMR in Molecular Biology*; Academic Press: New York, 1981.

monomer half-height line width in the presence of exchange, $\Delta\nu_{1/2}^M$ is the monomer half-height line width in the absence of exchange, and k_{MD} is the rate of exchange from the monomer to the dimer state.

As described by Mayo and Chen,⁷ greater than 90% monomer state exists at pH 3.2 and relatively low PF4 concentrations, whereas greater than 90% tetramer state is found at the same pH at higher PF4 concentrations. Under conditions where only monomer (low PF4 concentrations) or tetramer (higher PF4 concentrations) state is apparent,⁷ line widths are mostly unaffected by addition of these low TFE concentrations (data not shown); therefore, any additional line broadening must be due to the subunit exchange process. For the monomer Y60 3,5 ring proton resonance in the apparent absence of exchange, the line width is 12 Hz, while for the tetramer Y60 3,5 resonance 22 Hz is found. For the monomer state at the PF4 concentration used for data shown in Figure 1, but in the absence of TFE, exchange broadening adds 6 Hz (difference between $\Delta\nu_{1/2}$ and $\Delta\nu'_{1/2}$ in eq 2) to Y60 ring proton resonance line widths, yielding a jump rate out of the monomer state of 18 s^{-1} . For the tetramer species, the difference between $\Delta\nu_{1/2}$ and $\Delta\nu'_{1/2}$ in the absence of TFE is only about 1 Hz; from eq 2, this yields a flux rate out of the tetramer state of about 3 s^{-1} . As described by Chen and Mayo,⁸ the monomer–monomer association rate constant can be calculated from monomer–dimer–tetramer steady-state populations and the total PF4 concentration. The ratio of steady-state populations of two exchanging states is equal to the ratio of their two jump rates. Therefore, having steady-state populations and one jump rate gives the other jump rate. From the equilibrium constant and the dissociation jump rate, the association rate constant can be derived. In the absence of TFE, the monomer association rate constant⁸ is $1.6 \times 10^5\text{ M}^{-1}\text{ s}^{-1}$.

In the slow to moderately slow (or slow–intermediate) NMR exchange regime, which exists prior to resonance coalescence (see Figure 1), eq 2 allows PF4 subunit exchange rates to be calculated. In Figure 4 these values have been plotted versus the natural logarithm of TFE concentration as activation free energies, ΔG^*_{MD} , in the context of transition-state theory using eq 3 ac-

$$\Delta G^*_{MD} = -RT \ln (k_{MD}h/k_B T) \quad (3)$$

ording to Laidler,¹⁵ where R is the universal gas constant, T is the temperature in Kelvin, k_{MD} is the monomer–monomer association jump rate, h is Planck's constant, and k_B is the Boltzmann constant. A linear relationship between ΔG^*_{MD} and TFE concentration is evident with a slope of 0.5. A range for the Smoluchowski–Stokes–Einstein free energy of association, ΔG^*_{SM} , is indicated at the bottom of the figure, and an approximate ΔG^*_{MD} value at the NMR fast exchange limit (assumes k_{MD} of 1000 s^{-1}) is also indicated on the extrapolated linear curve. Interestingly, this estimated fast exchange limit value for ΔG^*_{MD} falls at about 12% TFE. If we use a k_{MD} value of 500 s^{-1} for the NMR fast exchange limit, the corresponding ΔG^*_{MD} value would fall at about 8% TFE. This latter value approaches TFE concentrations where NMR spectra (Figure 1) indicate the actual onset of the fast exchange regime, i.e., no apparent exchange-induced line broadening, at about 7% TFE.

Discussion

The association rate constant is, among other factors, directly related to the frequency of diffusional encounter between reactants. The greater the frequency of encounter is, then the larger the rate constant is. The simplest geometry with which to describe diffusional association is that of two uniformly reactive hard spheres. This model is most often cited in the literature and collectively may be called the Smoluchowski–Stokes–Einstein relation. The bimolecular association rate constant, k_a , for two spherical molecules that are identical, i.e., two PF4 monomer subunits, is given by the Smoluchowski equation^{9,16}

$$k_a = 4\pi(2D)(2r) = 16\pi Dr \quad (4)$$

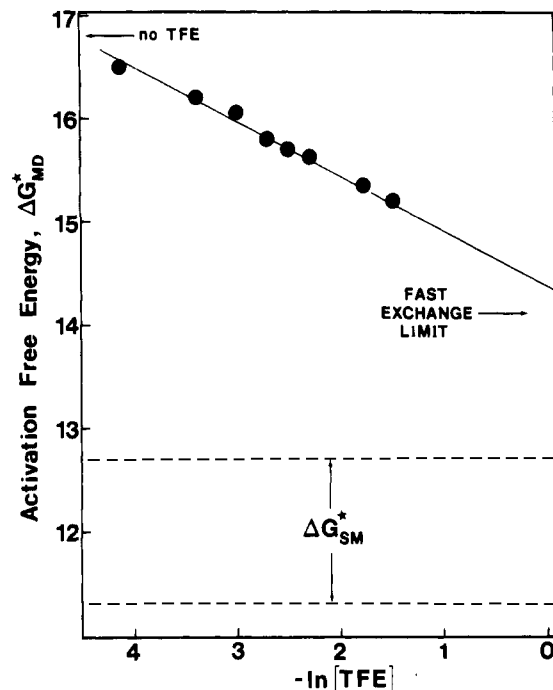


Figure 4. PF4 association activation free energy vs TFE concentration. Activation free energy for PF4 monomer–monomer association, ΔG^*_{MD} , calculated by using eq 3 is plotted versus the natural logarithm of TFE concentration. Values are given only for the slow to slow–intermediate exchange regime as discussed in the text. At the top of the figure, an arrow indicates ΔG^*_{MD} in the absence of TFE. ΔG^*_{MD} estimated at the NMR fast exchange limit, i.e., 1000 s^{-1} , is also indicated. At the bottom of the figure, a range for the Smoluchowski–Stokes–Einstein activation free energy, ΔG^*_{SM} , is shown bound by dashed lines.

where D is the diffusion constant and r is the molecular radius of interaction. For this hard-sphere case, the Stokes–Einstein relation¹⁷ gives

$$D = k_B T / (6\pi\eta a) \quad (5)$$

where $k_B T$ is the Boltzmann constant multiplied by the absolute temperature, η is the solvent viscosity, and a is the hydrodynamic radius of the molecule. Therefore, for two identical interacting molecules, $k_a = 8k_B T r / 3\eta a$. For PF4 monomer–monomer association, the Smoluchowski–Stokes–Einstein equation gives a value for k_a of about 10^8 – $10^9\text{ M}^{-1}\text{ s}^{-1}$. This value is most often taken as the maximum diffusion-limited association rate constant for molecular interactions of equal particle size.

In the absence of TFE, the rate constant for PF4 monomer–monomer association⁸ (k_{MD}) is in the range of $1 \times 10^5\text{ M}^{-1}\text{ s}^{-1}$, or about 3–4 orders of magnitude below the Smoluchowski diffusion limit. The PF4 monomer–monomer association rate constant is consistent with experimental rate constants observed for other similar molecular weight protein–protein associations. Melittin dimer and tetramer association rate constants¹⁸ are $(1\text{--}3.8) \times 10^5\text{ M}^{-1}\text{ s}^{-1}$. α -Chymotrypsin dimer association has a rate constant^{19,20} of 3.7×10^3 to $1.3 \times 10^3\text{ M}^{-1}\text{ s}^{-1}$. Insulin associates with its membrane-bound receptor with a rate constant^{21,22} of 1.6×10^5 to $2 \times 10^6\text{ M}^{-1}\text{ s}^{-1}$. Epidermal growth factor–receptor association²³ yields a value of $1.2 \times 10^6\text{ M}^{-1}\text{ s}^{-1}$. These values exemplify typical differences found between experiment and the Smoluchowski–Stokes–Einstein diffusion theory.

(16) Noyes, R. M. *Prog. React. Kinet.* **1961**, *1*, 129–150.

(17) Hynes, J. T. *Annu. Rev. Phys. Chem.* **1985**, *36*, 573–585.

(18) Schwarz, G.; Beschiaschvili, G. *Biochemistry* **1988**, *27*, 7826–7831.

(19) Kitano, H.; Maeda, Y.; Okubo, T. *Biophys. Chem.* **1989**, *33*, 47–54.

(20) Koren, R.; Hammes, G. G. *Biochemistry* **1975**, *15*, 1165–1173.

(21) Lipkin, E. W.; Teller, D. C.; De Haëns, C. *J. Biol. Chem.* **1986**, *261*, 1702–1711.

(22) Corin, R. E.; Donner, D. B. *J. Biol. Chem.* **1982**, *257*, 104–110.

(23) Mayo, K. H.; Nunez, M.; Burke, C.; Starbuck, C.; Lauffenburger, D.; Savage, C. R., Jr. *J. Biol. Chem.* **1989**, *264*, 17838–17844.

(15) Laidler, K. J. *Theories of Chemical Reaction Rates*; R. E. Krieger Publishing Co., Inc.: Huntington, NY, 1979; pp 41–55.

In fact, it is not too surprising that actual protein-protein association rate constants are so different from this diffusion limit. Many factors that influence molecular diffusional association have been omitted from the hard-sphere Stokes-Einstein diffusion model: steric/orientational, electrostatic, hydrodynamic effects, and even protein internal motions (protein dynamics). Due to these complications, biomolecular reactions may be diffusion controlled and yet have rate constants that differ by several orders of magnitude from what is expected on the basis of the simple Smoluchowski-Stokes-Einstein relations.²⁴⁻²⁶

When TFE is added to the PF4 solution and its concentration is increased, PF4 monomer association jump rates are monotonically increased from 18 to 180 s⁻¹ (slow-intermediate NMR exchange regime) and then above this value as the system is driven to, and then probably past, the NMR fast exchange limit of about 1000 s⁻¹. Since the PF4 concentration is unchanged, this increase in the jump rate is directly proportional to an increase in the protein-protein association rate constant, which can be calculated from knowledge of the PF4 concentration and steady-state monomer-dimer-tetramer population distributions as discussed by Mayo and Chen⁷ and by Chen and Mayo.⁸ The factorial change is about 2 orders of magnitude, and the corresponding PF4 association rate constant is now in the 10⁷ M⁻¹ s⁻¹ range. Therefore, it can be said that TFE effectively drives PF4 monomer association toward the Smoluchowski-Stokes-Einstein diffusion limit. Moreover, TFE is highly effective at relatively low concentrations.

While many solutes/solvents are known to disrupt protein aggregation and various charged solutes, like salts, are known to affect electrostatic contributions to either protein association or dissociation reactions,¹⁰ this is the first example of an organic solute with such a dramatic effect on protein-protein association. Often at considerably higher concentrations than used here, alcohols can denature proteins by the "binding" of their hydrophobic methyl and methylene groups to hydrophobic residues in the protein.^{27,28} At these relatively low concentrations, TFE apparently does not denature PF4 as judged by a linear relation between ΔG^*_{MD} and $\ln [\text{TFE}]$ and by mostly unchanging aggregate steady-state populations in the slow to slow-intermediate exchange regime where aggregate state resonances can still be resolved. Moreover, at 10% TFE the most downfield shifted α -CH and NH resonances (relative to HDO resonance) assigned to protons in antiparallel β -sheet conformations, while somewhat shifted and narrowed, are

present in the same spectral region showing the same 2D NMR spectral patterns (Chen and Mayo, unpublished results). These observations suggest that no major structural perturbations have occurred on addition of these concentrations of TFE. Moreover, polyhydric compounds like glycerol, for example, are known to stabilize protein structure by preferentially hydrating the protein molecule.²⁹ TFE also has been known for some time to stabilize peptide structure (normally at much higher concentrations) and may behave in a fashion similar to that of glycerol.

In the context of transition-state theory, an activation free energy barrier, ΔG^*_{MD} , of 16.8 kcal/mol for PF4 association in the absence of TFE is monotonically decreased by addition of TFE to about 14 kcal/mol at the NMR fast exchange limit. TFE reduces the presumably diffusion-controlled energy barrier by about 3 kcal/mol, bringing it closer to the Smoluchowski-Stokes-Einstein range. This result is quite surprising. The decrease in activation free energy should somehow be related to a change in the magnitude of the diffusion constant, D . According to eq 5, two variables, i.e., solvent viscosity and hydrodynamic radius, influence D . While the hydrodynamic radius could be affected somewhat by the addition of TFE, it is unlikely to vary by 2 orders of magnitude needed to explain these results. Most of the effect, therefore, probably lies in the viscosity term. The dependence of viscosity on solvent composition, however, can be quite complex, and a simple explanation cannot be given at this time. From this study it is evident that further experimental and theoretical investigations are necessary to elucidate the mechanism responsible for the sizable influence that TFE and perhaps other yet to be identified organic solutes have on protein molecular diffusion. Understanding why TFE perturbs molecular association dynamics so dramatically should add to our knowledge of how proteins, and biomolecules in general, interact and react in aqueous solution.

Abbreviations. PF4, platelet factor 4; TFE, trifluoroethanol; DSS, sodium 4,4-dimethyl-4-silapentanesulfonate; NMR, nuclear magnetic resonance; M-Y60, tyrosine-60 in the monomer state; D-Y60, tyrosine-60 in the dimer state; T-Y60, tyrosine-60 in the tetramer state.

Acknowledgment. This work was supported by a grant from the National Heart, Lung & Blood Institute (HL-43194) and benefitted from NMR facilities made available to Temple University through Grant RR-04040 from the National Institutes of Health. This work was completed in partial fulfillment of the Ph.D. requirements of Temple University for S.B.

Registry No. PF₄, 37270-94-3; TFE, 75-89-8.

(24) Berg, O. G.; von Hippel, P. H. *Annu. Rev. Biophys. Biophys. Chem.* **1985**, *14*, 131-140.

(25) Calef, D. F.; Deutch, J. M. *Annu. Rev. Phys. Chem.* **1983**, *34*, 493-501.

(26) Keizer, J. *Acc. Chem. Res.* **1985**, *18*, 235-241.

(27) Inoue, H.; Timasheff, S. N. *J. Am. Chem. Soc.* **1968**, *90*, 1890-1897.

(28) Inoue, H.; Timasheff, S. N. *Biopolymers* **1971**, *11*, 737-743.

(29) Gekko, K.; Timasheff, S. N. *Biochemistry* **1981**, *20*, 4667-4676.